Protein Farnesyl Transferase Target Selectivity Is Dependent upon Peptide Stimulated Product Release†

Jerry M. Troutman,‡ Douglas A. Andres,‡ and H. Peter Spielmann*,‡,§,||

Department of Molecular and Cellular Biochemistry, Department of Chemistry, and Kentucky Center for Structural Biology, University of Kentucky, Lexington, Kentucky 40536-0084

Received March 14, 2007; Revised Manuscript Received July 19, 2007

ABSTRACT: Protein farnesyl transferase (FTase) catalyzes transfer of a 15 carbon farnesyl lipid to cysteine in the C-terminal Ca_1a_2X sequence of numerous proteins including Ras. Previous studies have shown that product release is rate limiting and is dependent on binding of either a new peptide or isoprenoid diphosphate substrate. While considerable progress has been made in understanding how FTase distinguishes between related target proteins, the relative importance of the two pathways for product release on substrate selectivity is unclear. A detailed analysis of substrate stimulated product release has now been performed and provides new insights into the mechanism of FTase target selectivity. To clarify how FTase selects between different Ca_1a_2X sequences, we have examined the competition of various peptide substrates for modification with the isoprenoids farnesyl diphosphate (FPP) and anilinogeranyl diphosphate (AGPP). We find that reactivity of some competing peptides is correlated with apparent $K_m^{peptide}$, while the reactivity of others is predicted by the selectivity factor apparent $k_{cat}/K_m^{peptide}$. The peptide target selectivity also depends on the structure of the isoprenoid donor. Additionally, we observe two peptide substrate concentration dependent maxima and substrate inhibition in the steady-state reaction which require a minimum of three peptide binding states for the steady-state FTase reaction mechanism. We propose a model for the FTase reaction mechanism that, in addition to FPP stimulated product release, incorporates peptide binding to the FTase−FPP complex and the formation of an FTase−product−peptide complex followed by product release leading to an inhibitory FTase−peptide complex as a natural consequence of catalysis to explain these results.

The protein prenyltransferases, farnesyltransferase (FTase[1]) and geranylgeranyltransferase type I (GGTase-I), are zinc metalloenzymes that catalyze the first and obligatory step in a series of ordered post-translational modifications that direct protein membrane localization (*1*−*4*). FTase and GGTase-I catalyze the transfer of a 15- or 20-carbon isoprenoid, respectively, from farnesyl diphosphate (FPP, **1**, Figure 1) or geranylgeranyl diphosphate (GGPP) to form a thioether with a conserved Cys residue four amino acids from the C-terminus of target proteins (*5*−*8*). Protein substrates for both FTase and GGTase-I contain a Ca_1a_2X group at their C-terminus, where C is a conserved Cys residue, a_1 and a_2 are often aliphatic amino acids, and X is frequently M, Q, or S for FTase and L or F for GGTase-I (*9*, *10*). However, there are overlapping Ca_1a_2X substrate specificities for the prenyltransferases, where some canonical GGTase I substrates can be farnesylated by FTase, and vice versa (*11*, *12*).

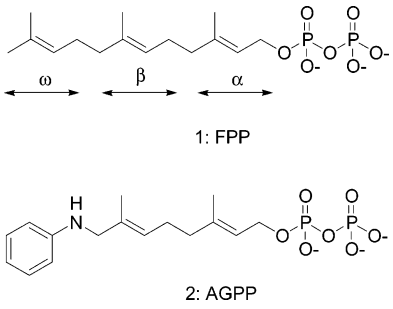

FIGURE 1: Structure of farnesyl diphosphate (**1**, FPP) and 8-anilinogeranyl diphosphate (**2**, AGPP).

The oncoprotein Ras must be prenylated both for membrane localization and to participate in cellular transformation (*13*). Constitutive activation of Ras is transforming in a wide variety of cell types, and mutations that activate Ras have been found in 30% of all cancers (*14*−*16*). A wide variety of other proteins with C-terminal Ca_1a_2X boxes have also been implicated in oncogenesis and tumor progression (*17*, *18*). Consequently, development of inhibitors of both FTase and GGTase-I are subjects of major drug discovery programs

† This work was supported in part by the Kentucky Lung Cancer Research Program (to H.P.S. and D.A.A.) and the National Institutes of Health (GM66152 to H.P.S.), and the NMR instruments used in this work were obtained with support from NSF CRIF Grant No. CHE-9974810.

* To whom correspondence should be addressed. Tel: 859-257-4790. Fax: 859-257-8940. E-mail: hps@uky.edu.

‡ Department of Molecular and Cellular Biochemistry.

§ Department of Chemistry.

|| Kentucky Center for Structural Biology.

[1] Abbreviations: FTase, protein farnesyltransferase; FPP, farnesyl diphosphate; GGTase-I, protein geranylgeranyltransferase type 1; GPP, geranyl diphosphate; GGPP, geranylgeranyl diphosphate; FTI, protein farnesyltransferase inhibitor; CaaX, tetrapeptide sequence cysteine−aliphatic amino acid−aliphatic amino acid−X (serine, glutamine, or methionine for FTase); dns, dansylated; RP-HPLC, reverse-phase high-performance liquid chromatography; H-Ras, Harvey-Ras; K-Ras, Kirsten-Ras; AGPP, 8-anilinogeranyl diphosphate; DTT, dithiothreitol; $^{app}k_{cat}$, apparent turnover number; $^{app}K_m^{peptide}$, apparent Michaelis−Menten constant for peptide.

10.1021/bi700513n CCC: $37.00
Published on Web 09/18/2007

Scheme 1: Generally Accepted FTase Kinetic Mechanism[a]

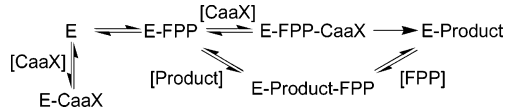

[a] E is the FTase enzyme, E-FPP is the FTase·FPP complex, E·FPP·CaaX is the FTase·FPP·CaaX peptide complex, E-Product is the FTase bound product complex, E-Product-FPP is the FTase bound to both FPP and the reaction product, and E-CaaX is the peptide bound FTase inhibitory complex.

(*19*, *20*). Several FTase inhibitors (FTIs) are currently in phase I, II, and III clinical trials for the treatment of cancer (*21*−*24*).

The currently accepted mechanism of the protein prenyltransferases is unexpectedly complex (Scheme 1) (*25*, *26*). Substrate association is assumed to proceed through a functionally ordered mechanism where FPP (**1**) first binds FTase, giving the enzyme·FPP complex (E·FPP) followed by Ca_1a_2X substrate association forming the enzyme·FPP·Ca_1a_2X peptide complex (E·FPP·CaaX) (*27*, *28*). After thioether formation, the modified peptide remains associated with FTase in an enzyme·product complex (E·product) (*28*, *29*). Product release is the rate determining step (k_{cat}) for the FTase reaction mechanism (*28*, *30*). An unusual feature of the FTase mechanism is that product dissociation is greatly enhanced by binding of either a new FPP or Ca_1a_2X peptide substrate (*29*). Apparently, two competing pathways can lead to the release of farnesylated peptide, depending on whether FPP or Ca_1a_2X peptide binds to the E·product complex. However, for the farnesylation of CVIM, FPP stimulates release slightly faster than does peptide (*29*). It is generally accepted in the literature that FPP is the substrate primarily responsible for stimulating product release (*29*, *31*). The steady-state kinetic constant k_{cat}/K_m is often used to describe the selectivity of an enzyme for its substrates (*32*). The apparent $k_{cat}/K_m^{peptide}$ is also the catalytic efficiency of FTase, and measures the ability of the enzyme to catalyze a reaction at low peptide substrate concentrations. Unlike the selectivity constant, catalytic efficiency does not depend on the competitive interaction of an alternative substrate target. In the case of FTase, the apparent $k_{cat}/K_m^{peptide}$ should describe FTase selectivity for different Ca_1a_2X peptide substrates (*10*, *31*). For example, apparent $k_{cat}/K_m^{peptide}$ for the H-Ras CVLS peptide is twice that measured for the K-Ras CVIM peptide. If apparent k_{cat} ($^{app}k_{cat}$) is dominated by FPP stimulated product release, apparent $k_{cat}/K_m^{peptide}$ should describe FTase selectivity. Therefore, the expected ratio of products from the farnesylation of two competing Ca_1a_2X substrates is given by eq 1,

$$\frac{V_a}{V_b} = \frac{\dfrac{V_{max_a} A e_t}{K_{m_a}\left(1 + \dfrac{B}{K_{m_b}}\right) + A}}{\dfrac{V_{max_b} B e_t}{K_{m_b}\left(1 + \dfrac{A}{K_{m_a}}\right) + B}} = \frac{\dfrac{k_{cat_a}}{K_{m_a}} A}{\dfrac{k_{cat_b}}{K_{m_b}} B} \qquad (1)$$

where k_{cat}/K_m is a selectivity factor, V_a and V_b are the rates of modification of the individual reaction components A and B, A and B are the concentrations of the reactants in the mixture, K_m is the Michaelis−Menten constant for each substrate, and e_t is the total enzyme concentration.

Interestingly, the ratio of products from the FTase catalyzed farnesylation of competing Ca_1a_2X peptides has not been reported. However, there are a number of reports suggesting that FPP binding may not be the sole, or even dominant, mechanism for product release (*10*, *25*, *29*, *30*). A crystal structure of FTase bound to both the farnesylated peptide and FPP (E·FPP·product) revealed that the product prenyl chain is displaced from the active site into an external hydrophobic groove ("exit groove") and the new FPP is bound in the active site (*25*). Surprisingly, the farnesylated peptide was not dissociated from the crystal by the presence of excess FPP. However, the farnesylated product was dissociated by additional peptide. Complicating matters further, Hartman et al. (*10*) found that some FTase reaction products do not dissociate from the enzyme even in the presence of excess FPP or peptide. However, the addition of a different, un-farnesylated Ca_1a_2X peptide stimulated product release. They go on to suggest that the enhanced farnesylation of one protein in the presence of a second protein substrate may be a novel regulatory mechanism. These observations are inconsistent with FPP stimulated product release as the sole mechanism for dissociation, and indicate that Ca_1a_2X substrate stimulated product release may also be important.

A wide range of Ca_1a_2X sequences have been identified as *potential* FTase substrates (*33*). However, farnesylation has only been confirmed for some of them. Understanding FTase substrate specificity may be critical for understanding which Ca_1a_2X motifs are farnesylated. Hartman et al. reported that the apparent $k_{cat}/K_m^{peptide}$ varies over 400-fold for 14 Ca_1a_2X peptides with different X-groups (*10*). However, it is unclear whether the product distribution for the competition of peptides for farnesylation by FTase will be adequately predicted by the apparent $k_{cat}/K_m^{peptide}$ since product release can potentially be stimulated by either of the two competing peptides or FPP (*29*).

The FTase reaction is unique because the FPP lipid moiety forms a substantial part of the binding surface for the target Ca_1a_2X peptide (*30*, *34*). Crystallographic studies of FTase with a bound Ca_1a_2X substrate and a nonhydrolyzable FPP analogue indicate that the ω-terminal isoprene unit of the lipid is in direct contact with the a_2 residue of the Ca_1a_2X motif (*30*, *35*). Unnatural FPP analogues with structures that differ from FPP may be useful in determining the molecular features of both the lipid and Ca_1a_2X peptide that contribute to the FTase mechanism (*31*, *36*−*38*). 8-Anilinogeranyl diphosphate (AGPP (**2**)) contains an aniline moiety which replaces the ω-terminal isoprene of FPP (*39*, *40*). AGPP is a good substrate for FTase with steady-state transfer constants apparent $K_m^{analogue}$ ($^{app}K_m^{analogue}$) and apparent $k_{cat}/K_m^{analogue}$ nearly identical to those of FPP (*39*, *40*). Recent studies with other FPP analogues have shown that the lipid structure can significantly affect the Ca_1a_2X target selectivity of the FTase enzyme (see companion manuscript, ref *53*) (*31*).

In this report, we measured the ability of FTase to selectively modify peptides corresponding to six different Ca_1a_2X motifs with the isoprenoid donors FPP and AGPP. The reactivity and the selectivity of FTase for the peptides were similar for both isoprenoid donors. Surprisingly, we found that the Ca_1a_2X substrate selectivity of the enzyme is

not predicted by the selectivity factor apparent $k_{cat}/K_m^{peptide}$ for all peptides. Rather, the ratio of products from competition reactions between some Ca_1a_2X peptides correlated with the ratio of ${}^{app}K_m^{peptide}$ instead of the apparent $k_{cat}/K_m^{peptide}$ ratios. We further analyzed the steady-state peptide dependent kinetics of the FTase reaction and found that there were at least three Ca_1a_2X substrate concentration dependent binding states in the FTase reaction mechanism. We propose that the binding states are due to peptide binding to the E·FPP complex, the E·product complex, and an E·CaaX substrate inhibition complex. These results demonstrate the importance of peptide stimulated product release in the mechanism of FTase and the involvement of this pathway in the selectivity of the FTase enzyme for different Ca_1a_2X targets.

EXPERIMENTAL PROCEDURES

General Experimental. AGPP and FPP were synthesized as described previously (*40*, *41*). All RP-HPLC was performed using an Agilent 1100 HPLC system equipped with a microplate autosampler, diode array, and fluorescence detector. The HPLC analysis was performed on a microsorb C18 column with 0.01% TFA in water (A) and 0.01% TFA CH_3CN (B) as the mobile phase. Peptides were purchased from Peptidogenics (Livermore, CA), and each contained a dansyl group N linked through a glycine linker to a Cys residue and then a variable a_1a_2X sequence (VLS, VIM, AHQ, RPQ, VIL, or KVQ). Spectrofluorometric analyses were performed in a 96-well black polystyrene, flat bottom, non-binding surface plate (excitation wavelength, 340 nm; emission wavelength 505 nm with a 10 nm cutoff) using a SpectraMax GEMINI XPS fluorescence well-plate reader. Absorbance readings were determined using a Cary UV/vis spectrophotometer. All assays were performed at minimum in triplicate. Recombinant mammalian (Rat) protein farnesyl transferase was a gift from Dr. Carol Fierke (University of Michigan).

Steady-State Peptide Kinetics. The steady-state kinetic constants ${}^{app}K_m^{peptide}$ and ${}^{app}k_{cat}$ with FPP and AGPP as isoprenoid donors and each dns-GCa_1a_2X peptide were determined in triplicate. The following assay components were assembled in individual wells of a 96-well plate and incubated at 30 °C for 20 min: total volume 300 μL containing 50 mM TrisHCl (pH 7.4), 12 mM $MgCl_2$, 12 μM $ZnCl_2$, 0.0167% *n*-dodecyl-β-D-maltoside (DM), 6.7 mM DTT, 6.7 μM isoprenoid diphosphate (FPP or AGPP from a 25 mM NH_4HCO_3 stock solution to give a final NH_4HCO_3 concentration of 0.8 mM), and *N*-dansyl-GCaaX peptide (variable concentrations, see below). Reactions were then initiated by the addition of FTase (final concentration 5 nM with the dns-GCLVS, dns-GCAHQ, dns-GCVIL, and dns-GCRPQ peptide, 10 nM with the dns-GCVIM peptide).

Final analysis peptide concentrations were chosen based on preliminary determination of the ${}^{app}K_m^{peptide}$ with 0.5, 1, 5, and 10 μM dns-GCa_1a_2X concentrations. Eight peptide concentrations were used in the final analysis: 0.17, 0.2, 0.25, 0.5, 0.75, 1, 2, and 3 times the estimated ${}^{app}K_m^{peptide}$ value with the dns-GCVLS, dns-GCAHQ, dns-GCVIL, dns-GCRPQ, and dns-GCKVQ peptides, and concentrations at 0.3, 0.45, 0.67, 0.9, 1.8, 2.7, 3.6, and 4.5 times the estimated ${}^{app}K_m^{peptide}$ for dns-GCVIM. Fluorescence was detected using a time based scan at 30 °C for 120 min or longer depending on when fluorescence enhancement ceased (see below). The velocity of each reaction was determined by converting the rate of increase in fluorescence intensity units (FLU/s) to μM/s with eq 2,

$$v_i = (RP)/(F_{max} - F_{min}) \quad (2)$$

where v_i is the velocity of the reaction in μM/s. R is the rate of the reaction in FLU/s. P is equal to the concentration of modified product in μM (see below). F_{max} is the fluorescence intensity of fully modified product. F_{min} is the fluorescence of a reaction mixture that contained 20 μL of assay buffer in the place of FTase.

Complete modification of peptides was assumed when fluorescence stabilized for more than 10 min and was confirmed by RP-HPLC analysis of the reaction mixture. If the reactions that contained higher concentrations of peptides did not go to completion, the $F_{max} - F_{min}$ value was extrapolated using a linear plot of the $F_{max} - F_{min}$ for each of the lower concentration reactions that did go to completion. Alternatively the extent of input peptide modified was determined by RP-HPLC analysis of the dansyl moiety peak absorbance corresponding to the unmodified and modified peptides. The percent of modified peptide relative to the total input peptide was then used to calculate the concentration of product in the mixture.

The velocities of the reactions were plotted against the concentration of peptide and were fit to the Michaelis−Menten equation (eq 3) to give the apparent k_{cat} (${}^{app}k_{cat}$) and $K_m^{peptide}$ (${}^{app}K_m^{peptide}$) values. The initial velocities used for the nonlinear fit were below the first V_{max}, and were the minimum number possible to give an error in the fit below 20%,

$$v_i/e_t = ({}^{app}k_{cat}[Pep])/({}^{app}K_m^{peptide} + [Pep]) \quad (3)$$

where e_t was the total enzyme concentration and [Pep] was the total input peptide.

Substrate Inhibition Analysis. The steady-state reaction profiles with high concentrations of peptide were analyzed as described above with peptide concentrations 4-, 5-, 6-, 7-, 8-, 9-, and 10-fold higher than the ${}^{app}K_m^{peptide}$.

Peptide Competition. Competition reactions were prepared with the same components given for the apparent $k_{cat}/K_m^{peptide}$ analysis except two peptides were added to the mixture. Peptide stock concentrations were measured by reading the Abs at 340 nm (ϵ^{dansyl} = 4250 $M^{-1}\cdot cm^{-1}$). All peptide competition reactions contained a final concentration of 3 μM for each peptide except the dns-GCVIM:dns-GCRPQ competition, which contained 1.5 μM dns-GCVIM and 4.5 μM dns-GCRPQ. Separate reactions were prepared as a standard with FPP or AGPP and only one peptide as described above. The reactions were initiated with the addition of FTase and analyzed spectrofluorometrically (reactions containing dns-GCVIM peptide used 20 nM final FTase concentration, and all others used 10 nM). The reactions were stopped prior to consumption of more than 50% of either peptide by adding 20 μL of a stop solution (isopropyl alcohol and acetic acid 4:1). HPLC analysis was then performed with 100 μL of the reaction mixture loaded onto a C18 column and eluted with a linear gradient of 0−30 min 10% B to 100% B at a flow rate of 1 mL/min. Peaks

Table 1: Kinetic Parameters $^{app}K_m^{peptide}$, $^{app}k_{cat}$, and Apparent $k_{cat}/K_m^{peptide}$ for dns-GCa_1a_2X Peptides with FPP or AGPP as the Isoprenoid Donor[a]

donor	peptide	$^{app}K_m^{peptide}$ (μM)	$^{app}k_{cat}$ (s^{-1}) $\times 10^{-2}$	apparent $k_{cat}/K_m^{peptide}$ ($\mu M^{-1}\cdot s^{-1}$) $\times 10^{-2}$
FPP	CVLS	0.8 ± 0.1	14 ± 2	18 ± 3
FPP	CVIM	0.30 ± 0.06	4.3 ± 0.5	14 ± 3
FPP	CAHQ	2.0 ± 0.3	20 ± 2	10 ± 2
FPP	CKVQ	1.5 ± 0.3	8 ± 1	5 ± 1
FPP	CVIL	6.6 ± 0.6	23 ± 2	3.5 ± 0.4
FPP	CRPQ	5 ± 1	8 ± 1	1.6 ± 0.4
AGPP	CVLS	0.5 ± 0.1	12 ± 2	24 ± 6
AGPP	CVIM	0.18 ± 0.06	1.6 ± 0.3	9 ± 3
AGPP	CAHQ	2.4 ± 0.5	21 ± 3	9 ± 2
AGPP	CKVQ	1.7 ± 0.2	11 ± 1	7 ± 1
AGPP	CVIL	16 ± 2	17 ± 1	1.1 ± 0.1
AGPP	CRPQ	10 ± 1	21 ± 2	2.1 ± 0.3

[a] Kinetic parameters $^{app}K_m^{peptide}$, $^{app}k_{cat}$, and apparent $k_{cat}/K_m^{peptide}$ for dns-GCa_1a_2X peptides with either 6.7 μM FPP or AGPP as the isoprenoid donor and varying concentrations of peptide in Tris-HCl buffer (pH = 7.4) plus reducing agent and detergent.

Table 2: HPLC Retention Time Comparison of Unmodified and Modified dns-GCa_1a_2X Peptides[a]

peptide substrate	t_R (min)		
	Ca_1a_2X	C(f)a_1a_2X	C(ag)a_1a_2X
CAHQ	5.5	15.7	10.9
CRPQ	5.8	16.1	11.4
CKVQ	6.2	16.2	11.4
CVLS	8.0	17.7	13.0
CVIM	9.6	18.8	14.4
CVIL	10.3	19.2	14.7

[a] HPLC retention times were measured using a C18 column and gradient elution with 0.01% TFA in water and acetonitrile (pH = 2.4) from 30% to 100% organic over 15 min. dns-GCAHQ, dns-GCRPQ, and dns-GCKVQ retention times were also measured in a pH = 7.4 PO_4^{3-} buffer with no change in the order of elution. The peptide hydrophobicity is increased by modification with either a farnesyl (C(f)a_1a_2X) or anilinogeranyl (C(ag)a_1a_2X) group. Note that the anilinogeranyl group is less hydrophobic than the farnesyl group.

on the 340 nm trace chromatogram that corresponded to both the standard reactions and fluorescent peaks were then integrated. The ratios of products were calculated according to eq 4,

$$(A_{mod}/A_{tot})/(B_{mod}/B_{tot}) \quad (4)$$

where A_{mod} is the integral of the modified peptide A, A_{tot} is the integral of the modified peptide A plus the unmodified peptide A, B_{mod} is the integral of the modified peptide B, and B_{tot} is the integral of the modified peptide B plus the unmodified peptide B. Alternatively, the ratios were calculated using the integrals of the standard peptide fluorescence relative to competition product fluorescence giving less than a 5% difference in the calculated ratio.

Overall Rate of Competition Reactions. The overall rate of the competition reaction was determined using the total amount of peptide modified as determined by RP-HPLC and eq 2. For one dns-GCVIM/dns-GCVLS peptide competition, a 1000 μL total volume reaction was sampled for RP-HPLC analysis every 45 min for 6 h.

Effect on Product Ratio of Increasing FPP and AGPP Concentrations. Competition reactions as described above with final FPP concentrations of 0.5, 1, 3, 6, 33, and 66 μM or AGPP concentrations of 0.5, 1, 10, 50, 200, and 400 μM were prepared to determine the effect of increasing isoprenoid concentration on the product ratios. FTase final concentrations were 10 nM for each reaction.

RESULTS

Individual CaaX Peptide Reactivity Is Similar with Both FPP and AGPP. In order to determine if apparent $k_{cat}/K_m^{peptide}$ is the selectivity factor for FTase, we measured the apparent $k_{cat}/K_m^{peptide}$ and $^{app}K_m^{peptide}$ for six dansylated-GCa_1a_2X (dns-GCa_1a_2X) peptides with saturating concentrations of the isoprenoids FPP and AGPP utilizing a continuous fluorescence assay (Table 1) (*10*, *39*, *42*, *43*). The steady-state kinetics of the K-Ras4B (CVIM) and H-Ras (CVLS) full length proteins and the corresponding Ca_1a_2X peptides with FPP have been extensively characterized (*10*, *28*, *31*, *44*−*46*). We confirmed that apparent $k_{cat}/K_m^{peptide}$ for the dansylated-GCVIM (dns-GCVIM) and dansylated-GCVLS (dns-GCVLS) substrates were identical to those previously reported in the literature (*31*, *46*). The other four substrates correspond to Ca_1a_2X motifs from physiologically important proteins, three of which are canonical FTase substrates: Cenp-F (dns-GCKVQ) (*47*), the DNAJ homologue, RDJ2 (dns-GCAHQ) (*48*), and the hepatitis delta virus (HDV) large antigen protein (dns-GCRPQ) (*49*), and the fourth, a canonical GGTase-I substrate Ca_1a_2X motif (dns-GCVIL) (*5*). These substrates range widely in structure and physical properties.

The catalytic efficiency (apparent $k_{cat}/K_m^{peptide}$) of the Ca_1a_2X substrates varied over a 11- and 22-fold range with FPP and AGPP, respectively (Table 1). The difference in reactivity of the peptides with each isoprenoid was similar, where dns-GCVLS was the most reactive peptide with both isoprenoids (Table 1). FTase showed slightly enhanced catalytic efficiency with AGPP relative to FPP for the dns-GCVLS, dns-GCVIM, and dns-GCRPQ peptides. Interestingly, the catalytic efficiency with the canonical GGTase-I substrate dns-GCVIL was decreased nearly 3-fold for AGPP relative to FPP.

Studies by Fierke and co-workers indicate that peptide selectivity for FTase over GGTase-I is determined in large part by the polarity and size of the X-residue (*10*). In particular, they showed that a series of dns-TKCVIX peptides with Q, S, and M terminal residues are good FTase substrates while those ending in L are not. In other work, we have shown that FTase peptide selectivity is dependent on both the a_2 and X-residues of the Ca_1a_2X motif (see companion paper, ref *53*). Interestingly, the three peptides in this study with Q X-residues all have different kinetic parameters (Table 1), suggesting that reactivity is also dependent on the identity of the a_1 and a_2 residues. The catalytic efficiency (apparent $k_{cat}/K_m^{peptide}$) of the six dns-GCa_1a_2X substrates was not correlated with the hydrophobicity of the peptides, even when the canonical GGTase-I substrate dns-GCVIL was removed from consideration (Table 2). The steady-state parameter apparent $k_{cat}/K_m^{peptide}$ for the reaction catalyzed by FTase includes the rate constants for the steps from peptide binding to E·FPP through farnesylation (Scheme 1). A critical step in the reaction is the rotation of the FPP prenyl chain to position C1 of the lipid near the Ca_1a_2X peptide sulfur nucleophile (*30*, *34*). It is possible that the observed differences in the kinetic parameters for the three Q X-terminal peptides are due to different interactions between the lipid and the a_1 and a_2 side chains of the peptide. These

Table 3: Competition of dns-GCa$_1$a$_2$X Peptide Pairs[a]

(a) With FPP as the Isoprenoid Donor

dns-GCa$_1$a$_2$X reactants		FPP				
peptide A	peptide B	product ratio fA:fB	apparent $k_{cat}/K_m^{peptide}$ ratio fA:fB	$^{app}K_m^{peptide}$ ratio fB:fA	$^{app}k_{cat}$ ratio fA:fB	best predictor of product ratio
CVIM	CVLS	2.3 ± 0.1	0.8 ± 0.2	2.7 ± 0.6	0.31 ± 0.06	$^{app}K_m^{peptide}$
CVIM	CRPQ	21.5 ± 0.1	9 ± 3	17 ± 5	0.54 ± 0.09	$^{app}K_m^{peptide}$
CAHQ	CRPQ	2.4 ± 0.3	6 ± 2	2.5 ± 0.6	2.5 ± 0.4	$^{app}K_m^{peptide}$
CVLS	CRPQ	5.0 ± 0.2	11 ± 3	6 ± 1	1.8 ± 0.3	$^{app}K_m^{peptide}$
CVLS	CKVQ	1.4 ± 0.2	3.6 ± 0.9	1.9 ± 0.4	1.8 ± 0.3	$^{app}K_m^{peptide}$
CVLS	CAHQ	1.8 ± 0.1	1.8 ± 0.5	2.5 ± 0.5	0.7 ± 0.1	$k_{cat}/K_m^{peptide}$
CKVQ	CAHQ	0.7 ± 0.1	0.5 ± 0.1	1.3 ± 0.3	0.4 ± 0.06	$k_{cat}/K_m^{peptide}$
CVIL	CRPQ	1.5 ± 0.3	2.2 ± 0.6	0.8 ± 0.2	2.9 ± 0.4	$k_{cat}/K_m^{peptide}$
CAHQ	CVIL	1.5 ± 0.2	2.9 ± 0.7	3.3 ± 0.6	0.9 ± 0.1	neither

(b) With AGPP as the Isoprenoid Donor

dns-GCa$_1$a$_2$X reactants		AGPP				
peptide A	peptide B	product ratio agA:agB	apparent $k_{cat}/K_m^{peptide}$ ratio agA:agB	$^{app}K_m^{peptide}$ ratio agB:agA	$^{app}k_{cat}$ ratio agA:agB	best predictor of product ratio
CVIM	CVLS	2.1 ± 0.1	0.4 ± 0.2	3 ± 1	0.13 ± 0.03	$^{app}K_m^{peptide}$
CVIM	CRPQ	23 ± 2	4 ± 2	60 ± 20	0.08 ± 0.02	between[b]
CAHQ	CRPQ	2.6 ± 0.1	4 ± 1	4 ± 1	1.0 ± 0.2	neither
CVLS	CRPQ	14.9 ± 0.3	11 ± 3	20 ± 4	0.6 ± 0.1	between[b]
CVLS	CKVQ	2.8 ± 0.8	3 ± 1	3.4 ± 0.8	1.1 ± 0.2	both
CVLS	CAHQ	2.4 ± 0.1	2.7 ± 0.9	5 ± 1	0.6 ± 0.1	$k_{cat}/K_m^{peptide}$
CKVQ	CAHQ	0.9 ± 0.1	0.7 ± 0.2	1.4 ± 0.3	0.52 ± 0.09	$k_{cat}/K_m^{peptide}$
CVIL	CRPQ	0.5 ± 0.1	0.52 ± 0.08	0.6 ± 0.1	0.81 ± 0.09	both

[a] Product ratios from reaction mixtures containing (a) FPP or (b) AGPP at 6.7 μM with two dns-GCa$_1$a$_2$X peptides at 3 μM each were measured by RP-HPLC analysis. Product was quantified by integration of 340 nm trace chromatogram. The best predictor of product ratio is indicated in the right-hand column as either apparent $k_{cat}/K_m^{peptide}$, $^{app}K_m^{peptide}$, neither, or both. Note that for the CVLS/CKVQ reaction with FPP, both the $^{app}k_{cat}$ and $^{app}K_m^{peptide}$ ratios are predictive. [b] The value of the product ratio is between the ratio of the apparent $k_{cat}/K_m^{peptide}$ and the ratio of the $^{app}K_m^{peptide}$.

differences may alter the prenyl chain rotation and/or the chemical farnesylation step.

Peptide Selectivity Is Not Predicted by the Ratio of Apparent $k_{cat}/K_m^{peptide}$. We performed competition reactions between pairs of dns-GCa$_1$a$_2$X peptides in order to determine whether apparent $k_{cat}/K_m^{peptide}$ is the selectivity factor for FTase. The products from competition reactions for pairs of dns-GCa$_1$a$_2$X peptides with either FPP or AGPP were separated by RP-HPLC and quantified by integration of the dansyl absorbance (Table 3). We were able to reliably quantify 15 pmol and greater of the dansyl absorbance corresponding to modified peptide in individual reactions. The equimolar 3 μM concentration of each peptide was used to remove concentration dependence from the product ratio and was sufficient to accurately determine the amount of product produced from each reaction without consuming more that 50% of either dns-GCa$_1$a$_2$X substrate. In most cases, the peptide concentrations were sufficiently high that the peptide substrates were expected to exhibit some degree of substrate inhibition with the exception of the dns-GCRPQ/dns-GCVIL, dns-GCAHQ/dns-GCVIL, dns-GCAHQ/dns-GCPRQ competition reactions (see below). Surprisingly, the ratio of products formed was not predicted from the ratio of the apparent $k_{cat}/K_m^{peptide}$ for most pairs of dns-GCa$_1$a$_2$X peptides examined (Table 3). The correct product distribution was predicted by the ratio of the apparent $k_{cat}/K_m^{peptide}$ for only seven of the 17 reactions examined.

Interestingly, the product distribution from eight of the reactions was correlated with the ratio of $^{app}K_m^{peptide}$. For example, a 4:5 product ratio of farnesyl-CVIM (fCVIM) to farnesyl-CVLS (fCVLS) was expected if apparent $k_{cat}/K_m^{peptide}$ is the selectivity factor for FTase (Table 3). Instead, we found a product ratio of 23:10 fCVIM:fCVLS (Table 3). The dns-GCVIM peptide was approximately 3-fold more competitive over the dns-GCVLS peptide than predicted by the ratio of apparent $k_{cat}/K_m^{peptide}$. We also found that the ratio of products was invariant for reactions where from 10% to 50% of the dns-GCVIM peptide was consumed. The correlation of product ratios of competition reactions for this subset of dns-GCa$_1$a$_2$X peptide pairs with the ratio of the $^{app}K_m^{peptide}$ gave a slope of 0.81 ($R = 0.98$) for FPP and a slope 1.3 for AGPP ($R = 0.99$) (Supporting Information Figure 1). In order for eq 1 to accommodate these observations, the ratio of $^{app}k_{cat}$ for the competing substrates must be equal to an isoprenoid dependent constant. However, inspection of the experimentally determined values for $^{app}k_{cat}$ (Table 1) indicates that this is not the case. Therefore, the isoprenoid dependent constants (0.81 for FPP and 1.3 for AGPP) must be due to some other factor(s). These results suggest that the mechanism of FTase is considerably more complex than previously appreciated.

Product Ratio Is Independent of Peptide Stoichiometric Ratio and Concentration. The failure of apparent $k_{cat}/K_m^{peptide}$ to predict the preferred substrate for the competition reactions between the CVIM/CVLS and CRPQ/CVIL peptide pairs at 3 μM each prompted us to examine the peptide concentration dependence of the product distribution. The $^{app}K_m^{peptide}$ for both the CRPQ and CVIL peptides with FPP is sufficiently high to allow accurate product quantification at substrate concentrations below, at, and above the $^{app}K_m^{peptide}$. We performed competition reactions between CRPQ and CVIL peptides at various stoichiometric ratios and concentrations and found that the product ratios were independent of both the peptide ratio and concentration (Table 4).

Table 4: Product Ratio for Competition Reaction with FPP between dns-GCVIL and dns-GCRPQ[a]

		dns-GCVIL/dns-GCRPQ	
dns-GCVIL (μM)	dns-GCVIL (μM)	stoichiometric ratio	ratio farnesylated products
3	3	1:1	1.5 ± 0.3
6	3	2:1	1.5 ± 0.1
1.5	3	1:2	1.3 ± 0.1
3	1.5	2:1	1.4 ± 0.1
3	6	1:2	1.3 ± 0.2
3	12	1:4	1.35 ± 0.04
6	6	1:1	1.62 ± 0.04

[a] Product ratio is independent of substrate stoichiometry and substrate concentration relative to $^{app}K_m^{peptide}$. Reactions were prepared at the following concentrations and analyzed by RP-HPLC as described in the Table 2 legend.

Product Ratio Is Dependent on the Isoprenoid Donor Concentration. The mechanism for FTase shown in Scheme 1 has two isoprenoid diphosphate bound states involved in product formation and release with an experimental apparent $K_m^{isoprenoid}$ for both FPP and AGPP of 46 nM for the dns-GCVLS (1 μM) peptide. The correlation of the product ratios from some of the competition experiments with an isoprenoid dependent ratio of the $^{app}K_m^{peptide}$ suggested the possibility of a more complex dependence of the reaction on isoprenoid diphosphate concentration. However, as the isoprenoid concentrations used in the competition reactions were well above apparent saturation for the isoprenoid donor, we did not expect any change in the product ratios with increasing concentration of isoprenoid diphosphate. To clarify these observations, we measured the product ratio from the reaction of dns-GCVIM and dns-GCVLS peptides over a range of FPP and AGPP concentrations (Figure 2). Surprisingly, the product ratio decreased with increasing concentrations of the isoprenoid donor, trending toward the ratio expected from eq 1. These unanticipated results suggest that the mechanism shown in Scheme 1 is incomplete.

Overall Rate of Competition Reactions Is Governed by the Rate of the Peptide with the Lowest $^{app}K_m^{peptide}$. To further characterize the peptide dependence of the observed product ratios, we examined the overall velocity of the competition reactions relative to the velocity of reactions for the individual peptides. The product distributions from competition reactions between the dns-GCVIM and dns-GCVLS peptides with both FPP and AGPP are not predicted by the ratio of apparent $k_{cat}/K_m^{peptide}$; rather they correlate with the ratio of $^{app}K_m^{peptide}$ (Table 2). For both isoprenoid diphosphates, the dns-GCVIM has both a lower $^{app}K_m^{peptide}$ and rate of transfer than dns-GCVLS. We found that the overall reaction rates of competition reactions between the dns-GCVIM and dns-GCVLS peptides with both FPP and AGPP as the isoprenoid donor were the same as for the dns-GCVIM peptide alone.

In contrast, the product distribution from competition reactions between the dns-GCKVQ/dns-GCAHQ and dns-GCRPQ/dns-GCVIL peptide pairs with AGPP correlates with the ratio of apparent $k_{cat}/K_m^{peptide}$. Competition reactions between the dns-GCKVQ/dns-GCAHQ and dns-GCRPQ/dns-GCVIL peptide pairs with AGPP as the isoprenoid donor were run in parallel with the corresponding single peptide reactions at the same individual substrate concentrations (Figure 3). This set of peptides and AGPP as the isoprenoid donor were chosen because the $^{app}K_m^{peptide}$ of each was very close, yet the individual reaction rates at 3 μM peptide concentration were sufficiently different to allow determination of which peptide had the largest effect on the overall rate of the competition reaction. We found that the overall rate of the dns-GCKVQ/dns-GCAHQ competition reaction was the same as for the reaction of the dns-GCKVQ peptide alone. Of the pair, the dns-GCKVQ peptide has the lower $^{app}K_m^{peptide}$ and the slower reaction rate. Similarly, the overall rate of the dns-GCRPQ/dns-GCVIL reaction was the same as for the lower $^{app}K_m^{peptide}$ dns-GCRPQ substrate alone. However, under these conditions, the reaction rate of the dns-GCRPQ peptide is higher than that of the dns-GCVIL. For all of the peptide pairs reported in Table 3, we found that the overall rate of reaction was that of the peptide with the lowest $^{app}K_m^{peptide}$. For example, competition between dns-GCVIM and dns-GCRPQ with AGPP proceeds at the rate of the reaction of dns-GCVIM with AGPP. In this reaction, the ratio of $^{app}K_m^{peptide}$ is approximately 60 and the major product is modified dns-GCVIM with very little modified dns-GCRPQ formation. These observations suggest that the overall rate of the competition reactions is governed by the rate of the peptide with the lowest $^{app}K_m^{peptide}$.

There Are a Minimum of Three Peptide Binding States in the FTase Steady-State Reaction. In the generally accepted FTase mechanism shown in Scheme 1, FPP association with the E·product complex is solely responsible for stimulating product release (*29*−*31*). As noted above, Ca_1a_2X peptides can stimulate product release, suggesting that peptide also interacts with the E·product complex. In addition, high concentrations of full length proteins and Ca_1a_2X peptides slow the FTase reaction (*46*, *50*). Presumably, this substrate inhibition occurs either due to slow formation of the E·CaaX complex to an active E·FPP·CaaX complex or due to the requirement for Ca_1a_2X dissociation from E·CaaX prior to FPP binding. In order to characterize Ca_1a_2X peptide stimulated product release, we investigated the FTase reaction using peptide concentrations higher than those required to reach maximum velocity. Much to our surprise, we found that increasing concentrations of the dns-GCKVQ substrate in reactions with both FPP and AGPP had more complex effects than simple inhibition (Figures 4a and 4b). As previously reported, the reaction rate increased to a maximum, before falling as the concentration of peptide was increased. Surprisingly, at even higher concentrations of peptide, the rate again increased slightly to a second, smaller maximum before finally approaching zero. To our knowledge, the second peptide concentration dependent rate increase has not been previously described. To confirm these observations, we examined the FTase reaction for the dns-GCa_1a_2X concentration dependence of the dns-GCVLS and dns-GCAHQ peptides with FPP (Figures 4c and 4d). The appearance of two peptide substrate concentration dependent maxima in these reaction profiles was similar to what we observed for dns-GCKVQ. The second rate maximum for the dns-GCVLS peptide was less pronounced than for dns-GCKVQ. Interestingly, with increasing concentrations of dns-GCAHQ we found that the rate dipped slightly after the first maximum and then rose gradually to a second, higher maximum before decreasing. Similar trends were observed with FPP and the peptides CVIM, CRPQ, and CVIL (see Supporting Information Figure 1).

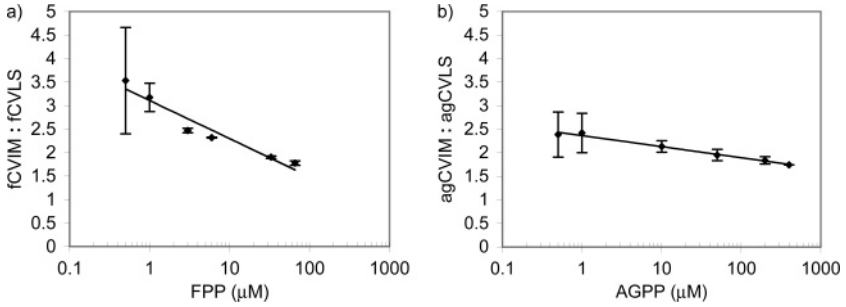

FIGURE 2: FTase competition product ratio is affected by isoprenoid concentrations. dns-GCVIM/dns-GCVLS peptide pair product ratios were measured from reaction mixtures containing 3 μM of the dns-GCVIM and dns-GCVLS peptide with (a) FPP or (b) AGPP at increasing concentrations. Note that the effect of increasing concentration of FPP on the product ratio is much greater than the effect with increasing AGPP concentrations. Also note that both plots are semilogarithmic and that the line is for illustrative purposes only.

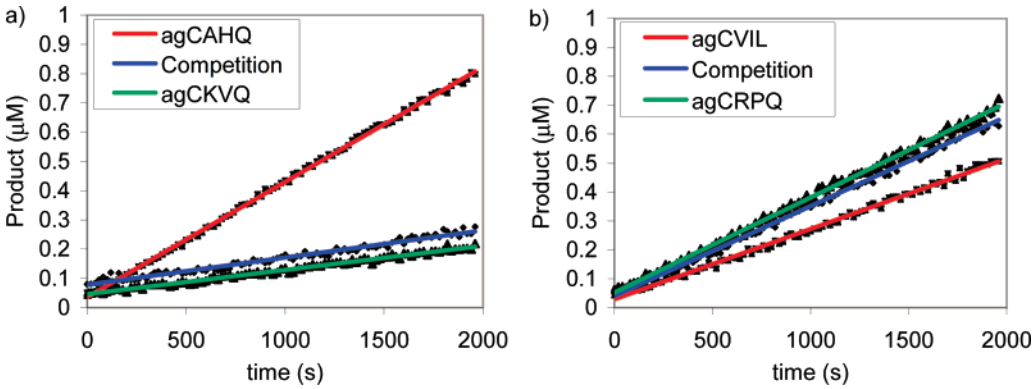

FIGURE 3: Overall rate of the competition reaction (blue) is governed by the rate of individual peptide reaction (red and green) with the lowest $^{app}K_m^{peptide}$ (green). Reactions were prepared that contained the peptide pair indicated in parallel with each individual peptide reaction at the same enzyme and peptide concentration. Data is the average of triplicate assays. (a) Competition of dns-GCAHQ and dns-GCKVQ peptides for AGPP modification. (b) Competition of dns-GCAHQ and dns-GCKVQ peptides for AGPP modification. Note that the rates of the competition reactions (blue) are the same as the rates of the single peptide reaction where the peptide is the one with the lowest apparent $K_m^{peptide}$ (green).

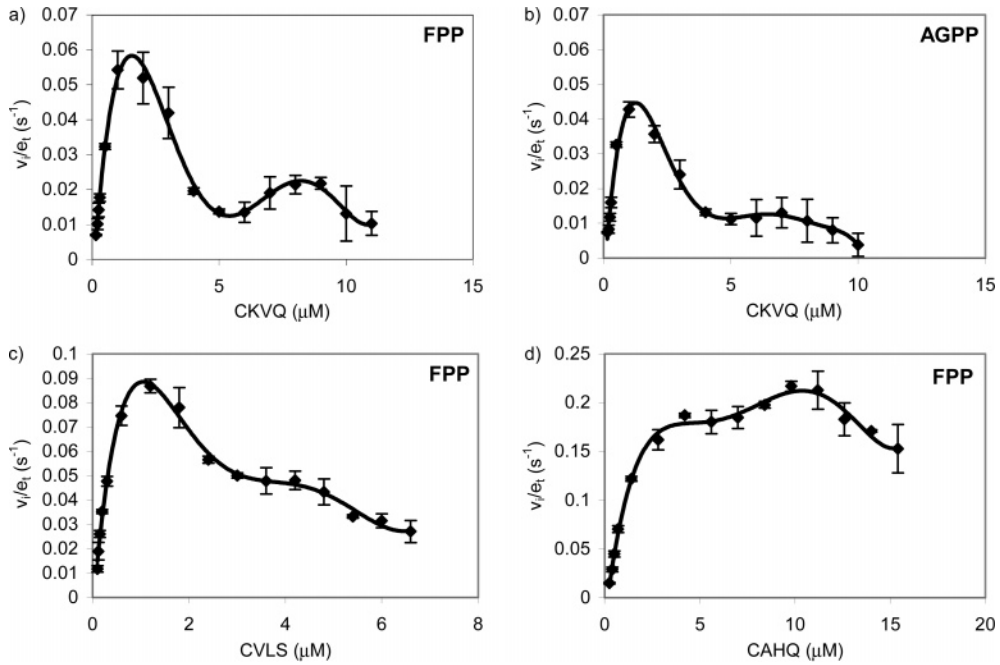

FIGURE 4: Steady-state inhibition reaction indicates three peptide binding states with (a) FPP + dns-GCKVQ, (b) AGPP + dns-GCKVQ, (c) FPP + dns-GCVLS, and (d) FPP + dns-GCAHQ. Reaction velocities were measured as described in Table 1. Note the second increase in the reaction rate after the first V_{max} point has been reached. Also note that the *y*-axis and *x*-axis scales are different with different peptides and that the lines are for illustrative purposes only. v_i/e_t is the initial rate divided by the enzyme concentration.

The effect of the dns-GCa_1a_2X peptide sequence on the relative $^{app}K_m^{peptide}$ and apparent $K_i^{peptide}$ for the FTase reaction with FPP is illustrated in Table 1 and Figures 4a, 4c, and 4d. The $^{app}K_m^{peptide}$ for these substrates is not simply the affinity of the peptide for E·FPP. It has previously been shown that the rate of the FTase reaction is not dependent

Scheme 2: Extended FTase Reaction Mechanism Incorporating Peptide Stimulated Product Release[a]

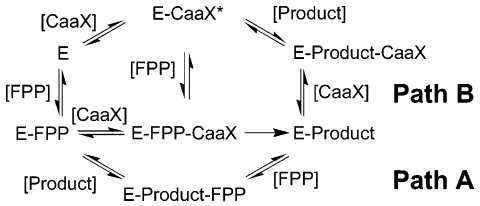

[a] The mechanism is split into two pathways with path A resulting in FPP stimulated product release and path B resulting in peptide stimulated product release. E is the FTase enzyme, E-FPP is the FTase·FPP complex, E·FPP·CaaX is the FTase·FPP·CaaX peptide complex, E-Product is the FTase bound product complex, E-Product-FPP is the FTase bound to both FPP and the reaction product, and E-CaaX is the peptide bound FTase inhibitory complex. E-Product-CaaX is the new peptide bound enzyme product complex. *E·CaaX formation slows the overall rate of the FTase reaction due to either the slow binding of FPP to give an active E·FPP·CaaX complex or requirement for the CaaX peptide to dissociate to give free enzyme prior to FPP binding.

on or correlated with the affinity of the Ca_1a_2X peptide for the E·FPP complex (*10*, *31*). For example, Fierke and coworkers have shown that dns-TKCVIQ is greater than 400 times more efficiently turned over than dns-TKCVIL but has a 10-fold lower affinity for E·FPP. Rather, $K_m^{peptide}$ is a more complex parameter that includes E·FPP·CaaX formation as well as the interaction of the Ca_1a_2X peptide with both FTase and the E·product complex. The peptide concentration required to reach the second maximum in the transfer reaction is negatively correlated with apparent peptide hydrophobicity (Table 2, Figures 4a, 4c, 4d). Previous reports have highlighted the importance of the X-residue in FTase selectivity and reactivity (*8*, *10*, *51*, *52*). While both dns-GCKVQ and dns-GCAHQ share the same X-residue, they have very different reactivity. These results provide further evidence that FTase substrate reactivity is dependent on the identities of all three terminal residues in the Ca_1a_2X peptide.

The presence of two peptide substrate concentration dependent maxima and substrate inhibition in the steady-state reaction profile requires a minimum of three peptide binding states. The generally accepted mechanism (Scheme 1) has only two peptide bound states (*42*, *50*). The second peptide bound state, E·CaaX, is thought to result from dissociation of FPP from the E·FPP complex, followed by peptide binding to FTase (*30*, *50*). Previous reports have shown that E·CaaX is nonproductive and is unable to bind FPP to form the reactive E·FPP·CaaX complex (*27*, *28*). Rather, the productive E·FPP complex is generated by peptide dissociation from E·CaaX followed by FPP binding. In this model, formation of the inhibitory E·CaaX requires peptide to out-compete FPP for association with the free enzyme. However, FPP has a much higher affinity for FTase than do the Ca_1a_2X peptides, and CVLS peptide affinity for E·FPP is 70-fold higher than for the free enzyme (*34*). Also, the E·FPP complex is highly committed toward catalysis since FPP dissociates at a rate 2.5 times slower than k_{cat} (*27*).

Here we propose a more complex model for the FTase reaction mechanism that takes these observations into account (Scheme 2). In common with the generally accepted mechanism, the first peptide bound state is the E·FPP·CaaX complex. The second state is the E·product·CaaX complex which is responsible for peptide stimulated product release. This state is formed in competition with E·product·FPP. Release of product from the E·product·CaaX complex would leave the third state, E·CaaX. In this scheme, product dissociation from E·product·CaaX (Scheme 2) would form the inhibitory E·CaaX complex as a natural consequence of catalysis. Additionally, higher concentrations of Ca_1a_2X peptide will drive formation of the inhibitory E·CaaX complex at the expense of E·FPP by favoring formation of E·product·CaaX relative to E·product·FPP without requiring dissociation of FPP from E·FPP. The experimental results are consistent both with FPP binding to the inhibitory E·CaaX to form the first peptide bound state E·FPP·CaaX and with dissociation of the CaaX peptide from E·CaaX to give free enzyme. While the data are insufficient to distinguish between these models, the high affinity of both FPP and Ca_1a_2X peptides for FTase suggests that formation of free enzyme is unlikely in reactions performed under conditions of saturating substrate. These results provide a possible explanation for how a full length protein can bind to FTase alone without requiring FPP to disassociate from the E·FPP complex (*27*).

Competition by two Ca_1a_2X peptides for the E·product complex suggests a mechanistic explanation for the observations that the peptide with the lowest $^{app}K_m^{peptide}$ controls the overall FTase reaction rate. In this scheme, the overall rate will depend on the relative affinity of the peptides and isoprenoid diphosphate for the E·product complex, as well as the rate of product release from the E·product·CaaX and E·product·FPP complexes. If one of the competing peptides binds the E·product complexes more efficiently and/or stimulates faster product release from E·product·CaaX, then its rate will determine the overall rate. Consequently, the $^{app}k_{cat}$ for both peptides in eq 1 will be the same. Second, increasing isoprenoid will compete with the peptides for E·product and increase flux through path A of Scheme 2. Consequently, the ratio of products formed under high concentrations of isoprenoid donor in a competition reaction between two peptides will be less dependent on peptide stimulated release. These conclusions are consistent with the experimental findings that the peptide with the lowest measured $^{app}K_m^{peptide}$ determines the overall rate and that, in some cases, the ratio of $^{app}k_{cat}$ for each of the competing substrates will be equal to an isoprenoid dependent constant.

Figure 2 shows that, at low isoprenoid concentrations, the product distribution of competition reactions between dns-GCVLS and dns-GCVIM for both FPP and AGPP are at the ratios predicted by the ratio of their $^{app}K_m^{peptide}$. In both cases, as the isoprenoid donor concentration increases, the ratio of products decreases and trends to that predicted by the ratio of the selectivity factors. While the behaviors of FPP and AGPP are similar, they are not identical. At low AGPP concentrations, the ratio of modified dns-GCVIM to dns-GCVLS is approximately 2.5, the ratio of the two peptides' $^{app}K_m^{peptide}$. However, the trend of the product ratio toward the ratio of the selectivity factors with increasing AGPP concentration is proportionally less than it is with FPP, suggesting that FPP stimulates product release more efficiently than AGPP (Figure 2). The measured $^{app}K_m^{peptide}$ for dns-GCKVQ is almost the same for reaction with FPP and AGPP (Table 1). However, inspection of Figure 4a and 4b indicates that the concentration for dns-GCKVQ inhibition is lower for AGPP than it is for FPP. These results are

consistent with AGPP being less efficient than FPP at stimulating product release and there being greater flux through the peptide stimulated release pathway at comparable isoprenoid concentrations. Crystal structures of the E·FPP and E·product·FPP complexes indicate that the isoprenoid in both complexes binds to the same hydrophobic surface in the enzyme active site (*30*). Incorporation of the aromatic ring and heteroatom into AGPP decreases its hydrophobicity relative to the isosteric farnesol, and the difference in polarity between the two molecules may account for the relatively higher efficiency of FPP stimulated product release. Therefore, the product distributions from competition reactions containing AGPP and multiple peptides would likely be more dependent on peptide stimulated product release than a FPP competition reaction under similar conditions.

DISCUSSION

Role of Peptide Stimulated Product Release in Specificity. We examined the functional importance of peptide stimulated product release in the reaction catalyzed by FTase. The efficient product release stimulated by peptide was unexpected given the reported preference of FTase for FPP mediated product release (*29*). We found that the rate constant for product release is sensitive to the structure of both the prenyl diphosphate and peptide substrates. The flux through the FPP and peptide stimulated release pathways is likely to depend on the relative binding affinity of the peptide or isoprenoid to the E·product complex as well as the rate of product dissociation from the corresponding E·product·substrate complexes. Under competition conditions this scheme becomes even more complex due to additional routes for product release made possible by association of alternative peptide substrates. It is also possible that peptide binding affinity to the E·product complex depends on the Ca_1a_2X sequence of the isoprenylated product bound in the active site of the enzyme. These observations can be interpreted to suggests an explanation for why ${}^{app}K_m{}^{peptide}$ is reported to be uncorrelated with K_d for Ca_1a_2X association with E·FPP (*10*, *31*). By incorporation of path B (Scheme 2) into the mechanism, ${}^{app}K_m{}^{peptide}$ also includes the affinity of peptide for E·product and the decomposition of E·product·CaaX. Therefore, depending on the properties of the Ca_1a_2X substrate, the steady-state parameter apparent $k_{cat}/K_m{}^{peptide}$ may not predict protein selectivity by FTase.

AGPP Alters FTase Target Preference. Changes in the structure of the isoprenoid will alter the interactions between the isoprenoid and the Ca_1a_2X peptide which may change the preference of the enzyme for different Ca_1a_2X substrates. Surprisingly, FPP and AGPP were similar in reactivity for most of the Ca_1a_2X sequences except the canonical GGTaseI target Ca_1a_2X sequence (dns-GCVIL). With FPP as the isoprenoid donor, FTase preferred the dns-GCVIL substrate over the dns-GCRPQ sequence. However, with AGPP as the isoprenoid donor, the enzyme preferred the dns-GCRPQ sequence over the dns-GCVIL peptide. Previous structural analyses with multiple Ca_1a_2X peptides in an E·inhibitor·CaaX complex (where the inhibitor was a nontransferable FPP analogue) indicated that canonical GGTaseI target peptides bind to FTase in a different conformation than canonical FTase substrates (*25*). The canonical FTase substrates bind to the E·FPP complex with the X residue bound to what is termed the "specificity pocket" and the ω-isoprene interacts directly with the a_2 residue of the Ca_1a_2X sequence. Interestingly, the canonical GGTase-I target sequence X-residue binds to a different site partially made up of the a_2 residue of the Ca_1a_2X peptide and the ω-isoprene of FPP. In AGPP the ω-isoprene of FPP is replaced with an aniline moiety. The difference in the binding conformation and interaction with the X-residue of the dns-GCVIL peptide may account for the difference in the ability of AGPP to react with the dns-GCVIL peptide.

Endogenous FTI Clearance. FTase and GGTase-I catalyze prenylation of proteins with distinct, but partially overlapping, sets of Ca_1a_2X motifs, where many of the canonical GGTase-I target peptides are poor substrates for FTase and *vice versa* (*11*, *12*). The identity of the C-terminal residue of the Ca_1a_2X sequence is an important determinant of the *in vivo* protein substrate preferences of the two enzymes (*9*, *10*). An investigation into the role of the C-terminal X-residue revealed that a wide range of Ca_1a_2X peptide substrates for both enzymes had consistently high affinity for both the FTase and GGTase-I E·FPP complexes (*10*). A consequence of this high affinity is that GGTase-I substrate Ca_1a_2X peptides can efficiently bind to the FTase·FPP complex and undergo chemistry to form farnesylated products that are slowly turned over. In extreme cases, Ca_1a_2X substrates with very slow product release may act as FTIs. A particularly dramatic example is the dns-TKCVIL peptide which undergoes a single turnover where the farnesylated product is not released from the active site even in the presence of FPP or excess dns-TKCVIL peptide (*10*). Interestingly, this product inhibition is relieved by the addition of a second Ca_1a_2X peptide (dns-TKCVIC) to the dns-TKCVIL E·product complex. The possibility exists that some of the approximately 700 putative proteins with Ca_1a_2X motifs found in the human genome may also act as product inhibitors of the FTase reaction (*33*). Such naturally occurring FTIs may slow farnesylation of important cellular proteins, suggesting that peptide stimulated product release may be an important mechanism to allow tightly bound farnesylated Ca_1a_2X peptides to be cleared from the FTase active site (*10*).

ACKNOWLEDGMENT

We thank Dr. Carol Fierke, Katherine Hicks, and Heather Hartman for the gift of mammalian rat protein farnesyltransferase, helpful discussions, and help with the kinetic assay development. We thank Dr. Isaac Wong and Dr. Louis B. Hersh for helpful discussions on the enzyme kinetics.

SUPPORTING INFORMATION AVAILABLE

Figure comparing the ratio of products with ${}^{app}K_m{}^{peptide}$ and figure depicting steady-state inhibition reaction indicating three peptide binding states with (a) FPP + CVIM, (b) FPP + CVIL, (c) FPP + CRPQ, (d) AGPP + CVIM, (e) AGPP + CVIL, (f) AGPP + CRPQ, (g) AGPP + CVLS, and (h) AGPP + CAHQ. This material is available free of charge via the Internet at http://pubs.acs.org.

REFERENCES

1. Zhang, F. L., and Casey, P. J. (1996) Protein prenylation: molecular mechanisms and functional consequences, *Annu. Rev. Biochem. 65*, 241−269.
2. Adjei, A. A. (2003) An overview of farnesyltransferase inhibitors and their role in lung cancer therapy, *Lung Cancer 41* (Suppl. 1), S55−S62.

3. Rowinsky, E. K., Windle, J. J., and Von Hoff, D. D. (1999) Ras protein farnesyltransferase: A strategic target for anticancer therapeutic development, *J. Clin. Oncol. 17*, 3631−3652.
4. Vergnes, L., Peterfy, M., Bergo, M. O., Young, S. G., and Reue, K. (2004) Lamin B1 is required for mouse development and nuclear integrity, *Proc. Natl. Acad. Sci. U.S.A. 101*, 10428−10433.
5. Moores, S. L., Schaber, M. D., Mosser, S. D., Rands, E., O'Hara, M. B., Garsky, V. M., Marshall, M. S., Pompliano, D. L., and Gibbs, J. B. (1991) Sequence dependence of protein isoprenylation, *J. Biol. Chem. 266*, 14603−10410.
6. Roskoski, R., Jr. (2003) Protein prenylation: a pivotal posttranslational process, *Biochem. Biophys. Res. Commun. 303*, 1−7.
7. Dunten, P., Kammlott, U., Crowther, R., Weber, D., Palermo, R., and Birktoft, J. (1998) Protein Farnesyltransferase: Structure and Implications for Substrate Binding, *Biochemistry 37*, 7907−7912.
8. Caplin, B. E., Ohya, Y., and Marshall, M. S. (1998) Amino acid residues that define both the isoprenoid and CAAX preferences of the Saccharomyces cerevisiae protein farnesyltransferase. Creating the perfect farnesyltransferase, *J. Biol. Chem. 273*, 9472−9479.
9. Reiss, Y., Stradley, S. J., Gierasch, L. M., Brown, M. S., and Goldstein, J. L. (1991) Sequence requirement for peptide recognition by rat brain p21ras protein farnesyltransferase, *Proc. Natl. Acad. Sci. U.S.A. 88*, 732−736.
10. Hartman, H. L., Hicks, K. A., and Fierke, C. A. (2005) Peptide specificity of protein prenyltransferases is determined mainly by reactivity rather than binding affinity, *Biochemistry 44*, 15314−15324.
11. Armstrong, S. A., Hannah, V. C., Goldstein, J. L., and Brown, M. S. (1995) CAAX geranylgeranyl transferase transfers farnesyl as efficiently as geranylgeranyl to RhoB, *J. Biol. Chem. 270*, 7864−7868.
12. Boutin, J. A., Marande, W., Petit, L., Loynel, A., Desmet, C., Canet, E., and Fauchere, J. L. (1999) Investigation of S-farnesyl transferase substrate specificity with combinatorial tetrapeptide libraries, *Cell Signal 11*, 59−69.
13. Michaelson, D., Ali, W., Chiu, V. K., Bergo, M., Silletti, J., Wright, L., Young, S. G., and Philips, M. (2005) Postprenylation CAAX Processing Is Required for Proper Localization of Ras but Not Rho GTPases, *Mol. Biol. Cell 16*, 1606−1616.
14. Bos, J. L. (1989) ras oncogenes in human cancer: a review, *Cancer Res. 49*, 4682−4689.
15. Kloog, Y., and Cox, A. D. (2004) Prenyl-binding domains: potential targets for Ras inhibitors and anti-cancer drugs, *Semin. Cancer Biol. 14*, 253−261.
16. Gschwind, A., Fischer, O. M., and Ullrich, A. (2004) The discovery of receptor tyrosine kinases: targets for cancer therapy, *Nat. Rev. Cancer 4*, 361−370.
17. Adnane, J., Muro-Cacho, C., Mathews, L., Sebti, S. M., and Munoz-Antonia, T. (2002) Suppression of rho B expression in invasive carcinoma from head and neck cancer patients, *Clin. Cancer Res. 8*, 2225−2232.
18. de Bono, J. S., Tolcher, A. W., and Rowinsky, E. K. (2003) Farnesyltransferase inhibitors and their potential in the treatment of breast carcinoma, *Semin. Oncol. 30*, 79−92.
19. Gibbs, J. B., Oliff, A., and Kohl, N. E. (1994) Farnesyltransferase inhibitors: Ras research yields a potential cancer therapeutic, *Cell 77*, 175−178.
20. Karp, J. E., and Lancet, J. E. (2004) Farnesyltransferase inhibitors (FTIs) in myeloid malignancies, *Ann. Hematol. 83* (Suppl. 1), S87−S88.
21. Doll, R. J., Kirschmeier, P., and Bishop, W. R. (2004) Farnesyltransferase inhibitors as anticancer agents: critical crossroads, *Curr. Opin. Drug Discovery Dev. 7*, 478−486.
22. Woo, J. T., Nakagawa, H., Krecic, A. M., Nagai, K., Hamilton, A. D., Sebti, S. M., and Stern, P. H. (2005) Inhibitory effects of mevastatin and a geranylgeranyl transferase I inhibitor (GGTI-2166) on mononuclear osteoclast formation induced by receptor activator of NFkappaB ligand (RANKL) or tumor necrosis factor-alpha (TNF-alpha), *Biochem. Pharmacol. 69*, 87−95.
23. Gotlib, J. (2005) Farnesyltransferase inhibitor therapy in acute myelogenous leukemia, *Curr. Hematol. Rep. 4*, 77−84.
24. Santucci, R., Mackley, P. A., Sebti, S., and Alsina, M. (2003) Farnesyltransferase inhibitors and their role in the treatment of multiple myeloma, *Cancer Control 10*, 384−387.
25. Reid, T. S., Terry, K. L., Casey, P. J., and Beese, L. S. (2004) Crystallographic analysis of CaaX prenyltransferases complexed with substrates defines rules of protein substrate selectivity, *J. Mol. Biol. 343*, 417−433.
26. Sousa, S. F., Fernandes, P. A., and Ramos, M. J. (2005) Unraveling the mechanism of the farnesyltransferase enzyme, *J. Biol. Inorg. Chem. 10*, 3−10.
27. Pompliano, D. L., Schaber, M. D., Mosser, S. D., Omer, C. A., Shafer, J. A., and Gibbs, J. B. (1993) Isoprenoid diphosphate utilization by recombinant human farnesyl:protein transferase: interactive binding between substrates and a preferred kinetic pathway, *Biochemistry 32*, 8341−8347.
28. Furfine, E. S., Leban, J. J., Landavazo, A., Moomaw, J. F., and Casey, P. J. (1995) Protein farnesyltransferase: kinetics of farnesyl pyrophosphate binding and product release, *Biochemistry 34*, 6857−6862.
29. Tschantz, W. R., Furfine, E. S., and Casey, P. J. (1997) Substrate binding is required for release of product from mammalian protein farnesyltransferase, *J. Biol. Chem. 272*, 9989−9993.
30. Long, S. B., Casey, P. J., and Beese, L. S. (2002) Reaction path of protein farnesyltransferase at atomic resolution, *Nature 419*, 645−650.
31. Reigard, S. A., Zahn, T. J., Haworth, K. B., Hicks, K. A., Fierke, C. A., and Gibbs, R. A. (2005) Interplay of isoprenoid and peptide substrate specificity in protein farnesyltransferase, *Biochemistry 44*, 11214−11223.
32. Ferscht, A. R. (1999) *Structure and Mechanism in Protein Science: A Guide to Enzyme Catalysis and Protein Folding*, W. H. Freeman, New York.
33. Maurer-Stroh, S., and Eisenhaber, F. (2005) Refinement and prediction of protein prenylation motifs, *Genome Biol. 6*, R55.
34. Hightower, K. E., Huang, C.-c., Casey, P. J., and Fierke, C. A. (1998) H-Ras Peptide and Protein Substrates Bind Protein Farnesyltransferase as an Ionized Thiolate, *Biochemistry 37*, 15555−15562.
35. Long, S. B., Casey, P. J., and Beese, L. S. (2000) The basis for K-Ras4B binding specificity to protein farnesyltransferase revealed by 2 A resolution ternary complex structures, *Struct. Fold Des. 8*, 209−222.
36. Subramanian, T., Wang, Z., Troutman, J. M., Andres, D. A., and Spielmann, H. P. (2005) Directed library of anilinogeranyl analogues of farnesyl diphosphate via mixed solid- and solution-phase synthesis, *Org. Lett. 7*, 2109−2112.
37. Turek-Etienne, T. C., Strickland, C. L., and Distefano, M. D. (2003) Biochemical and structural studies with prenyl diphosphate analogues provide insights into isoprenoid recognition by protein farnesyl transferase, *Biochemistry 42*, 3716−3724.
38. Mu, Y., Gibbs, R. A., Eubanks, L. M., and Poulter, C. D. (1996) Cuprate-Mediated Synthesis and Biological Evaluation of Cyclopropyl- and tert-Butylfarnesyl Diphosphate Analogs, *J. Org. Chem. 61*, 8010−8015.
39. Chehade, K. A., Kiegiel, K., Isaacs, R. J., Pickett, J. S., Bowers, K. E., Fierke, C. A., Andres, D. A., and Spielmann, H. P. (2002) Photoaffinity analogues of farnesyl pyrophosphate transferable by protein farnesyl transferase, *J. Am. Chem. Soc. 124*, 8206−8219.
40. Chehade, K. A., Andres, D. A., Morimoto, H., and Spielmann, H. P. (2000) Design and synthesis of a transferable farnesyl pyrophosphate analogue to Ras by protein farnesyltransferase, *J. Org. Chem. 65*, 3027−3033.
41. Davisson, V. J., Woodside, A. B., and Poulter, C. D. (1985) Synthesis of allylic and homoallylic isoprenoid pyrophosphates, *Methods Enzymol. 110*, 130−144.
42. Cassidy, P. B., Dolence, J. M., and Poulter, C. D. (1995) Continuous fluorescence assay for protein prenyltransferases, *Methods Enzymol. 250*, 30−43.
43. Pompliano, D. L., Gomez, R. P., and Anthony, N. J. (1992) Intramolecular Fluorescence Enhancement - a Continuous Assay of Ras Farnesyl - Protein Transferase, *J. Am. Chem. Soc. 114*, 7945−7946.
44. Hicks, K. A., Hartman, H. L., and Fierke, C. A. (2005) Upstream polybasic region in peptides enhances dual specificity for prenylation by both farnesyltransferase and geranylgeranyltransferase type I, *Biochemistry 44*, 15325−15333.
45. Pickett, J. S., Bowers, K. E., Hartman, H. L., Fu, H. W., Embry, A. C., Casey, P. J., and Fierke, C. A. (2003) Kinetic studies of protein farnesyltransferase mutants establish active substrate conformation, *Biochemistry 42*, 9741−9748.
46. Pompliano, D. L., Rands, E., Schaber, M. D., Mosser, S. D., Anthony, N. J., and Gibbs, J. B. (1992) Steady-state kinetic mechanism of Ras farnesyl:protein transferase, *Biochemistry 31*, 3800−3807.
47. Ashar, H. R., James, L., Gray, K., Carr, D., Black, S., Armstrong, L., Bishop, W. R., and Kirschmeier, P. (2000) Farnesyl transferase

inhibitors block the farnesylation of CENP-E and CENP-F and alter the association of CENP-E with the microtubules, *J. Biol. Chem. 275*, 30451−30457.
48. Andres, D. A., Shao, H., Crick, D. C., and Finlin, B. S. (1997) Expression cloning of a novel farnesylated protein, RDJ2, encoding a DnaJ protein homologue, *Arch. Biochem. Biophys. 346*, 113−124.
49. O'Malley, B., and Lazinski, D. W. (2005) Roles of carboxyl-terminal and farnesylated residues in the functions of the large hepatitis delta antigen, *J. Virol. 79*, 1142−1153.
50. Dolence, J. M., Cassidy, P. B., Mathis, J. R., and Poulter, C. D. (1995) Yeast protein farnesyltransferase: steady-state kinetic studies of substrate binding, *Biochemistry 34*, 16687−16694.
51. Fiordalisi, J. J., Johnson, R. L., 2nd, Weinbaum, C. A., Sakabe, K., Chen, Z., Casey, P. J., and Cox, A. D. (2003) High affinity for farnesyltransferase and alternative prenylation contribute individually to K-Ras4B resistance to farnesyltransferase inhibitors, *J. Biol. Chem. 278*, 41718−41727.
52. Strickland, C. L., Windsor, W. T., Syto, R., Wang, L., Bond, R., Wu, Z., Schwartz, J., Le, H. V., Beese, L. S., and Weber, P. C. (1998) Crystal Structure of Farnesyl Protein Transferase Complexed with a CaaX Peptide and Farnesyl Diphosphate Analogue, *Biochemistry 37*, 16601−16611.
53. Troutman, J. M., Subramanian, T., Andres, D. A., and Spielmann, H. P. (2007) Selective modification of CaaX peptides with *ortho*-substituted anilinogeranyl lipids by protein farnesyl transferase: competitive substrates and potent inhibitors from a library of farnesyl diphosphate analogues, *Biochemistry 46*, 11310−11321.

BI700513N